Self-consistent Method for Determining Vertical Profiles of Aerosol and Atmospheric Properties Using a High Spectral Resolution Rayleigh–Mie Lidar

D. A. KRUEGER, L. M. CALDWELL, R. J. ALVAREZ II,* AND C. Y. SHE

Department of Physics, Colorado State University, Fort Collins, Colorado

(Manuscript received 4 January 1992, in final form 7 August 1992)

ABSTRACT

A self-consistent method of inverting high spectral resolution, Rayleigh–Mie lidar signals to obtain profiles of atmospheric state variables, as well as aerosol properties, is presented. Assumed are a known air pressure at a reference height, hydrostatic equilibrium, the ideal gas law, and the theoretical temperature and pressure dependence of Rayleigh–Brillouin line shapes. For measurements over several kilometers, variations in the atmospheric pressure must be included in the data analysis. The inversion of the signal is greatly facilitated by making a quadratic expansion of the line shape as a function of atmospheric temperature and pressure that is accurate for temperature ranges of ±30 K and pressure ranges of ±25 kPa around a standard temperature and pressure of 275 K and 76 kPa, respectively. Required measurements are the total lidar signal and signals corresponding to different portions of molecular scattering spectrum. These measurements are made possible by using interference filters and atomic vapor filters, which remove the aerosol contribution. The filters are fully characterized by measuring their transmission functions as a function of frequency. For a typical barium filter such as those considered here, the oven temperature must be controlled to better than 1 K for air temperature determination within 1 K. Specially designed filters will be less sensitive to filter temperature. If the bandwidth of the interference filters used is fairly broad, then the inclusion of rotational Raman scattering is important for accurate lidar inversion. Formulas for determining the vertical profiles of atmospheric temperature, pressure, and density, as well as backscatter ratio, backscatter phase function, extinction ratio, and aerosol extinction coefficient are given and their measurement sensitivities are discussed.

1. Introduction

Measurement of vertical profiles of aerosol optical properties and atmospheric temperatures are of considerable importance to atmospheric physics (Measures 1984). It is therefore one of the principal goals of lidar measurements in the troposphere to measure directly the backscatter ratio r_β and temperature profiles (She 1990) thereby determining all relevant vertical profiles of aerosol optical properties and the state variables of a troposphere in hydrostatic and local thermal equilibrium. Direct measurement of tropospheric temperature T (or air density n) profile with high spatial resolution and long ranges has not yet been demonstrated. Different lidar systems to date have obtained a partial evaluation of optical aerosol properties, often with assumptions on atmospheric state variables. Table 1 summarizes some of these methods and the parameters measured, where P is the pressure, α_a is the aerosol extinction coefficient, and PF is the phase function.

If a power law is used to relate the aerosol backscatter coefficient β_a to the corresponding extinction coefficient α_a, the profile of aerosol extinction coefficient can be obtained from the inversion of the broadband Rayleigh–Mie lidar signal (Klett 1981, 1986). Evans (1988) has discussed the variability of β_a/α_a as a function of aerosol properties. Since α_a at a reference location must be given, this inversion converges more rapidly in an optically thick atmosphere and is often used for measurement in a horizontal path. The aerosol mixing ratio profile has been determined by a broadband hybrid vibrational Raman and Rayleigh–Mie lidar (Melfi 1972). Using an air density (or temperature) profile from an independent source, the hybrid lidar signal can be used to determine the profile of aerosol extinction coefficient (Ansmann et al. 1990). Alternatively, it can be used to determine the temperature profile if the Klett inversion is used and β_a/α_a is assumed to be range independent (Kobayashi and Yamada 1988).

Keckhut et al. (1990) have demonstrated that a Rayleigh lidar enhanced to also measure Raman scattering from nitrogen can measure temperatures from 12 km up to nearly 100 km. Below that range, correcting for aerosol attenuation becomes a problem.

Since Rayleigh scattering can probe molecular scattering with a cross section three orders of magnitude larger than vibrational Raman scattering, the aerosol

* Current affiliation: Environmental Protection Agency, Division AMS, Las Vegas, Nevada.

Corresponding author address: Dr. David A. Krueger, Department of Physics, Colorado State University, Fort Collins, CO 80523.

TABLE 1. Comparison with other methods. All methods assume hydrostatic equilibrium and ideal gas law for air.

	Quantities required	Quantities obtained T	P	n	r_β	α_a	PF
This work	pressure at one reference height	×	×	×	×	×	×
Klett inversion (1981, 1986)	power law relating α_a and β_a extinction coefficients at the reference point					×	
Raman, (Ansmann et al. 1990)	use density (or temperature) profile from another measurement					×	
Raman with Rayleigh–Mie (Kobayashi and Yamada 1988)	use Klett inversion T and P at reference height backscatter/extinction = const	×	×	×	×		
HSRL–Wisconsin system (Shipley et al. 1983)	use density (or temperature) profile from another measurement pressure at one reference height	×	×		×	×	×

mixing ratio, in principle, can be measured more easily with Rayleigh–Mie scattering. However, since both Rayleigh (molecular) and Mie (aerosol) scattering are quasi-elastic, a narrowband system is necessary to disentangle their contributions (She 1990). Using a two-channel Fabry–Perot polyetalon interferometer, Shipley et al. (1983) have successfully separated light scattered from the atmosphere into its Doppler-broadened molecular and elastically scattered aerosol components. Their high spectral resolution lidar (HSRL) can be used to determine the backscatter ratio directly and deduce the aerosol extinction profile if the density (or temperature) is obtained from an independent source. Although the molecular channel of their instrument can only partially reject aerosol scattering due to the fundamental limitation of an interference spectrometer, exciting studies on atmospheric dynamics and cirrus clouds have been conducted using this system (Grund and Eloranta 1988). To separate the two scattering components more effectively, we have proposed (Shimizu et al. 1983) the use of atomic resonance blocking filters and have developed barium vapor filters with variable bandwidth for the rejection of aerosol scattering. The feasibility of such a resonance filter has been demonstrated in a preliminary laboratory experiment with a single-frequency continuous wave (cw) laser (Lehmann et al. 1986), and more recently in field measurements in which vertical atmospheric backscattering profiles were measured to 10% accuracy with analog detection (Alvarez et al. 1990).

Methods to measure the tropospheric temperature profile from lidar observations have been pursued actively over the past two decades. Rotational Raman scattering can be used to measure atmospheric temperature profiles (Cooney 1972, 1984; Arshinov et al. 1983) without the knowledge of the aerosol distribution. Since Raman scattering cross sections are relatively small, DIAL (differential absorption lidar) (Mason 1975) and HSRL–Rayleigh (Fiocco et al. 1971) techniques have been proposed for temperature measurements at longer ranges. In DIAL, the useful lidar signal depends on the comparison between Rayleigh–Mie scattering at wavelengths on and off an absorption peak of a chosen species. Although the use of differential absorption of two resonance lines is typical (Murray et al. 1980; Schwemmer and Wilkerson 1979), Kalshoven et al. (1981) recognized that near the ground, the fractional changes in temperature and the peak resonance absorption coefficient are proportional and were able to use a single O_2 absorption line near 770 nm to sense atmospheric temperature. Because of an intrinsic problem in range resolution, only an average temperature over a range of more than 1 km (Endemann and Byer 1981; Murray et al. 1980) has been determined with the DIAL technique. On the other hand, the HSRL–Rayleigh lidar does not have this intrinsic limitation in range resolution (She 1990). With the use of either interferometers (Schwiesow and Lading 1981) or atomic vapor filters (Shimizu et al. 1983), this technique, which has the advantage of high scattering cross section, has been proposed as a direct method to determine tropospheric temperatures. In the method using atomic vapor filters, the Rayleigh–Mie lidar signal is divided into two receiving channels, each passing through a narrowband rejection filter set to eliminate aerosol (Mie) scattering and to allow different portions of the molecular (Rayleigh) scattering spectrum to be detected. Atmospheric temperature is then determined by comparing the measured intensity ratio of the two channels to the corresponding calculated ratio, based on measured filter transmission functions and theoretical temperature- and pressure-dependent Rayleigh spectra (Tenti et al. 1974). Despite the attractiveness of the HSRL–Rayleigh technique, there is no tropospheric temperature profile measurement with high spatial resolution reported to date. After pursuing an experimental program using barium atomic vapor filters and the HSRL–Rayleigh technique for several years, we have come to the realization that the pressure dependence of the calculated Rayleigh scattering ratio, which has been ignored (Shimizu et al. 1983), should be included if the temperature profile is to be determined over an altitude of several kilometers. In addition, for a typical experimental setup for field mea-

surements to be discussed, the contribution due to rotational Raman scattering must be included.

The purpose of this paper is to present a self-consistent, iterative procedure for lidar inversion that incorporates the pressure dependence of the calculated Rayleigh scattering intensity ratio. With this procedure we show that, using the atmospheric pressure at a single reference altitude, the vertical profiles of temperature, density, and pressure of a troposphere in hydrostatic and local thermal equilibrium can be determined from our lidar data without any other assumptions. We also discuss the precision of temperature measurement in terms of sensitivity coefficients, which can be evaluated from the theoretical Rayleigh function and the measured characteristics of the atomic vapor filters. Combining the temperature–density profiles with the backscatter ratio profile allows us to determine the optical properties of the aerosols, that is, the profiles of aerosol extinction coefficient and phase function. A brief report using these techniques for a preliminary field experiment has been reported (She et al. 1992). A more extensive report on field experiments appears as a companion paper (Alvarez et al. 1993).

2. High spectral resolution lidar

A sketch of a HSRL is shown in Fig. 1. A narrowband laser pulse (0.1 GHz, 4.5 ns, 15 mJ) is scattered by the atmosphere (both molecules and aerosols), collected by a telescope, and split into two beams. Each of the beams passes through a barium atomic vapor filter and an interference filter and then is detected (Alvarez et al. 1990). The light backscattered by the molecules in the air is broadened to a full width at half-maximum (FWHM) of about 2.7 GHz at an atmospheric temperature of 275 K and pressure of 76 kPa. The molecular temperature is roughly proportional to the square of this width. The light scattered by the aerosols is also (Doppler) broadened but to less than 0.1 GHz because the velocity of the relatively massive aerosols is much smaller than a typical molecular velocity of 450 m s^{-1}. As will be shown, to obtain the air temperature within 1 K requires that the molecular scattering signal be determined to an accuracy of about 0.2%. This can be done without a knowledge of the aerosols if less than 1 part in 10^3 of the aerosol scattering passes through the filter (i.e., 30-dB rejection for a backscatter ratio of 4). To attain the accuracy of 0.2% requires that the barium atomic vapor filter temperature be stabilized to better than 1 K for typical filters. The laser is tuned first on and then off the barium absorption at 553.7 nm and scattered photons, N_{on} and N_{off}, respectively, are detected.

The transmission through a barium vapor filter (central temperature 755 K, argon buffer gas pressure = 10 torr = 1.3 kPa) as measured by scanning the narrowband pulsed laser is shown in Fig. 2a. In terms of the laser line-shape function $g_L(\nu)$ and the filter line-

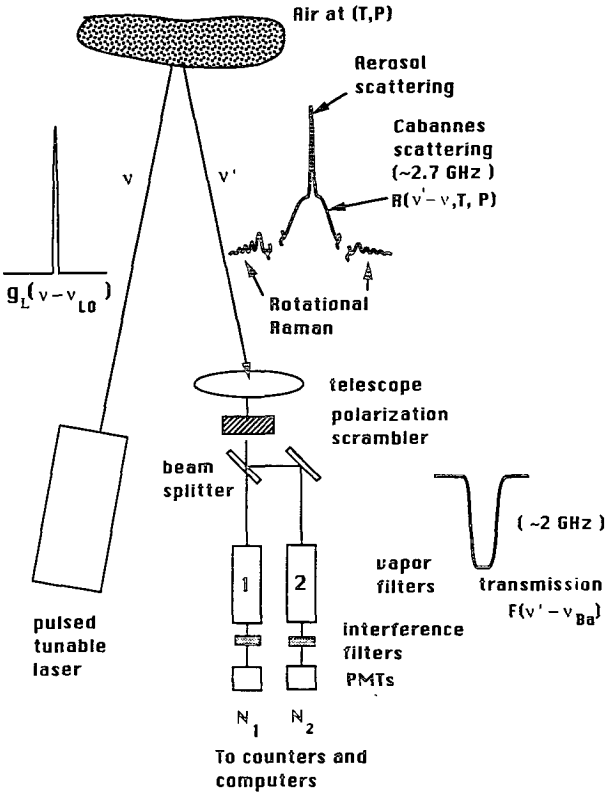

FIG. 1. Schematic of high spectral resolution lidar showing the narrowband (~0.13 GHz), pulsed, tunable laser source, the scattered spectrum with the narrow aerosol scattering peak and the broader Rayleigh–Brillouin molecular scattering (~2.7 GHz), the collecting telescope, the atomic barium vapor filters (~2 GHz), and the detectors. Not shown are the photon counting electronics and the computer for data storage and analysis.

shape function $F_0(\nu)$, the experimentally measured filter line shape is

$$F(\nu_{L0} - \nu_{Ba}) = \int g_L(\nu - \nu_{L0}) F_0(\nu - \nu_{Ba}) d\nu. \quad (1)$$

For our system the laser line-shape function $g_L(\nu)$ has a measured FWHM of about 0.13 GHz. The measured $F(\nu)$ appears in the following analysis, and it should be noted that it depends upon both the vapor filter and the characteristics of the light source.

Figure 1 includes a polarization scrambler that is assumed in the following analysis. It scrambles the received light and transmits equal intensities in two independent polarizations to the beam splitter. This avoids complications due to polarization effects at the beam splitter. Preliminary field experiments did not include the scrambler and these polarization effects are included in the data analysis (Alvarez et al. 1993). The interference filter blocks much of the background light from the sky as well as the blackbody radiation from the hot vapor filters from entering the photomultipliers.

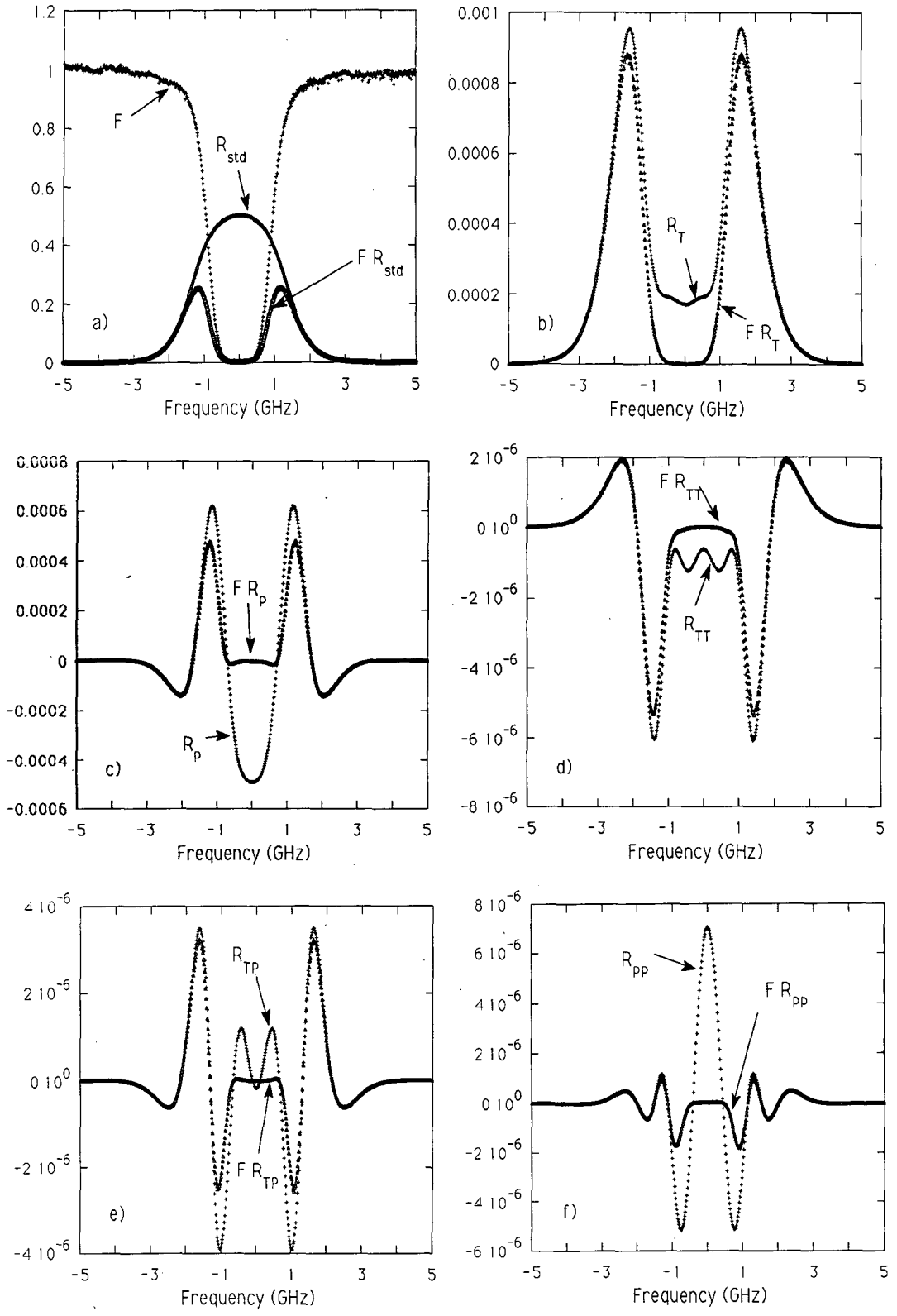

FIG. 2. (a) Transmission function $F(\nu)$ of barium filters for vapor temperature of 755 K, the Rayleigh–Brillouin line shape $R_{std}(\nu)$ for backscattering from air at $T = 275$ K and $P = 76$ kPa, and the product $F(\nu)R_{std}(\nu)$; (b) $R_T(\nu)$ and $F(\nu)R_T(\nu)$ (K^{-1}); (c) $R_P(\nu)$ and $F(\nu)R_P(\nu)$ (kPa^{-1}); (d) $R_{TT}(\nu)$ and $F(\nu)R_{TT}(\nu)$ (K^{-2}); (e) $R_{TP}(\nu)$ and $F(\nu)R_{TP}(\nu)$ ($K^{-1}\,kPa^{-1}$); and (f) $R_{PP}(\nu)$ and $F(\nu)R_{PP}(\nu)$ (kPa^{-2}). Note the different ordinate scales. The $R_\mu(\nu)$ functions are defined by Eq. (7).

3. Theory

For the laser tuned to the center of the barium absorption line, the basic lidar equation gives the number of photons returning from a range bin with length Δz at a range z and passing through a filter as

$$N_{on} = \frac{\mathcal{P}_{on}\Delta t}{h\nu}\frac{A}{z^2}\Delta z\xi_{on}(\nu, z)\beta_m \times \frac{f_m}{f_0}\exp\left[-2\int dz'\alpha(\nu, z')\right], \quad (2a)$$

where $\mathcal{P}_{on}$ is the average laser power, Δt is the time over which counts are accumulated, A is the telescope area, h is Planck's constant, and ν is the laser light frequency. The molecular backscattering coefficient is β_m. Since the bandwidth of our interference filters is about 20 nm, both the central component (Cabannes line) and rotational fine structure (now termed rotational Raman lines) of Rayleigh scattering (Young 1982) should be added to give a molecular backscatter coefficient of $\beta_m = \beta_R + \beta_{RR} = n(P, T)d\sigma/d\Omega$. With the laser tuned to the barium resonance frequency, the aerosol scattering is completely blocked, the central Rayleigh scattering (Cabannes line) is partially blocked, and rotational Raman scattering is unaffected by the atomic vapor filter. The much weaker vibrational Raman scattering, which is outside the pass band of the interference filter, is ignored. Thus, the effective backscattering coefficient may be written as

$$\beta_m\frac{f_m}{f_0} = \frac{f_R}{f_0}\beta_R + \beta_{RR}, \quad (2b)$$

with

$$f_m = \frac{f_R + \gamma f_0}{1 + \gamma}, \quad (2c)$$

where $\gamma = \beta_{RR}/\beta_R$. Since the molecular backscatter coefficients β_R, and β_{RR} are the products of molecular density $n(T, P)$ and respective molecular differential cross sections, γ is independent of altitude. The central Rayleigh attenuation factor is given by

$$f_R(T, P) = \int R(\nu, T, P)F(\nu)d\nu, \quad (2d)$$

which can be calculated from a laboratory measured transmission function of the atomic vapor filter $F(\nu)$ and the calculated Rayleigh–Brillouin scattering function $R(\nu, T, P)$, based on a theoretical six-moment model (S6) of Tenti et al. (1974). The normalization factor is

$$f_0(T) = \int R(\nu, T, P)d\nu = \left(\frac{2}{\lambda}\right)\left(\frac{2k_BT}{m}\right)^{1/2}, \quad (2e)$$

where λ, k_B, and m are, respectively, wavelength, Boltzmann constant, and average molecular mass of 28.9 amu. The extinction coefficient is

$$\alpha(z) = n(T, P)\sigma + \alpha_a, \quad (2f)$$

where σ is the total molecular cross section for air, and α_a is the aerosol extinction coefficient. The air temperature and pressure are T and P, respectively. The efficiency factor $\xi_{on}(\nu, z)$ includes the collection and detector efficiencies (giving a possible frequency dependence) and the overlap of the outgoing laser beam and the telescope viewing function (giving a z dependence). The exponential factor in (2a) gives the round-trip attenuation of the beam (assumed to be independent of frequency for the 10 GHz or so of frequency shift in going on and off the filter resonance). We have assumed that the light backscattered by the aerosol has been totally absorbed by the atomic vapor filter.

The number of photons that are not directed through the filter (or if the laser is tuned far off resonance where $F = 1$), consisting of both molecular and aerosol scattering contributions, is given by

$$N_{off} = \frac{\mathcal{P}_{off}\Delta t}{h\nu}\frac{A}{z^2}\Delta z\xi_{off}(\nu, z) \times (\beta_m + \beta_{a-})\exp\left[-2\int dz'\alpha(\nu, z')\right], \quad (3)$$

where β_a is the aerosol backscattering coefficient. Measurements of N_{on} and N_{off} allow us to determine properties of the aerosols and the atmosphere.

a. *Atmospheric properties*

A two-channel experiment makes use of two interference filters and two atomic vapor filters of different widths obtained by holding them at different temperatures. With the laser tuned to the barium resonance, the ratio of two on-resonance lidar signals will be

$$\frac{N_{1on}}{N_{2on}} = \frac{\mathcal{P}_{1on}\xi_{1on}f_{m1}}{\mathcal{P}_{2on}\xi_{2on}f_{m2}}. \quad (4)$$

Since N_{1on} and N_{2on} are measured simultaneously, the intensity ratio $\mathcal{P}_{1on}/\mathcal{P}_{2on} = 1$. For a given pressure, the ratio of two on-resonance signals, N_{1on}/N_{2on}, can be used to determine the atmospheric temperature if the ratio ξ_{1on}/ξ_{2on} is known, and the molecular attenuation factor ratio f_{m1}/f_{m2}, which is pressure and temperature dependent, can be assessed using (2c)–(2e) by independent measurement. The functions f_{R1} and f_{R2} are determined from $F_1(\nu)$ and $F_2(\nu)$, measured in the laboratory by passing laser beams through the filters, and from the theoretical values of the Rayleigh–Brillouin function $R(\nu, T, P)$. A correct value for the differential cross section ratio of the Rayleigh scattering components, $\gamma = \beta_{RR}/\beta_R$, is essential for the temperature calculation because a 1% error in γ will change the calculated temperature by approximately 1 K. The γ value of 0.0255 used for data analysis is deduced from the King correction factor of 1.049 for air given in a recent paper (Bates 1984). This γ value is in

agreement with the measured cross sections of pure rotational Raman scattering (Penney et al. 1974) and Rayleigh scattering (Shardanand and Rao 1977) for nitrogen and oxygen. The on-resonance efficiency ratio ξ_{1on}/ξ_{2on}, which may be altitude dependent if the z dependence of the telescope viewing functions for the two channels are different, cannot be determined directly under these experimental conditions. However, since the on- and off-resonance frequencies differ only by about 10 GHz, it is reasonable to assume that it is equal to the off-resonance efficiency ratio ξ_{1off}/ξ_{2off}, which can be measured directly. With the laser tuned off the barium resonance, a second experiment measures the off-resonance ratio of the intensities

$$\frac{N_{1off}}{N_{2off}} = \frac{\mathcal{P}_{1off}\xi_{1off}}{\mathcal{P}_{2off}\xi_{2off}}. \tag{5}$$

Again we can take $\mathcal{P}_{1off}/\mathcal{P}_{2off} = 1$, so this measurement determines ξ_{1off}/ξ_{2off}, which may be mildly dependent upon altitude z. Using (5) in (4) we obtain

$$\frac{N_{1on}}{N_{2on}} = \frac{N_{1off}(\xi_{1on}/\xi_{1off})f_{m1}(T, P)}{N_{2off}(\xi_{2on}/\xi_{2off})f_{m2}(T, P)}. \tag{6a}$$

Assuming that $(\xi_{1on}/\xi_{1off})(\xi_{2on}/\xi_{2off})^{-1}$ is not only independent of z but identically unity, we may simplify (6a) by defining $C_i = N_{ion}/N_{ioff}$ (i = 1 or 2) so

$$\frac{C_1}{C_2} = \frac{f_{m1}(T, P)}{f_{m2}(T, P)}. \tag{6b}$$

Equation (6b) is an implicit expression relating the air temperature and pressure to the measured signals since, as previously stated, the on-resonance filter ratio f_{m1}/f_{m2} can be determined independently. For this procedure, it is important to make sure that the laboratory laser beams, used to independently determine f_{m1} and f_{m2}, see the same filter transmission functions, $F_1(\nu)$ and $F_2(\nu)$, as the received lidar signals.

b. *Rayleigh–Brillouin function*

Central to the use of the lidar signals to deduce the atmospheric temperature profile is the inversion of (6) where the atmospheric temperature and pressure enter through the f_m factors. We have used the theoretical six-moment model of Tenti et al. (1974) for $R(\nu, T, P)$ for a diatomic gas of particles of mass $m = 4.81 \times 10^{-26}$ kg, internal specific heat k_B (= Boltzmann's constant), the combination of parameters (shear viscosity $\times$ k_B)(thermal conductivity $\times$ m)$^{-1}$ equaling 0.198, the ratio of the bulk viscosity to shear viscosity of 0.76, and for a wavelength of 553.7 nm. The lineshape for backscattering from air at 275 K and 76 kPa is shown in Fig. 2a. Since the direct calculations are somewhat involved and a real-time determination of the temperature profile is of interest, we have expanded $R(\nu, T, P)$ for temperatures and pressures in a range about a standard point (T_0 = 275 K, P_0 = 76 kPa) in terms of six functions of frequency

$$R(\nu, T, P) = R_{std}(\nu) + (T - T_0)R_T(\nu) + (P - P_0) \times R_P(\nu) + 0.5(T - T_0)^2R_{TT}(\nu) + (T - T_0) \times (P - P_0)R_{TP}(\nu) + 0.5(P - P_0)^2R_{PP}(\nu). \tag{7}$$

The coefficients R_μ, where μ takes on the values std, T, P, TT, TP, and PP, are just the value at the standard point and the derivatives of $R(\nu, T, P)$. At each frequency these six R_μ functions were obtained by calculating $R(\nu, T, P)$ on an array of 91 points in the (T, P) plane (245 K $\leq T \leq$ 305 K and 50 kPa $\leq P \leq$ 100 kPa) and then doing a least-squares fit to the form in (7). To calculate the molecular attenuation factors f_{R1} and f_{R2} for data analysis, it is convenient to define the coefficients $f_{\mu i}$ as

$$f_{\mu i} = \int R_\mu(\nu)F_i(\nu)d\nu, \tag{8}$$

and i = 1 or 2 identifies the filter. Typical values (for a 755-K filter) are f_{std} = 0.4159 GHz, f_T = 0.001917 GHz K^{-1}, $f_P = 2.16 \times 10^{-4}$ GHz kPa^{-1}, $f_{TT} = -1.57 \times 10^{-6}$ GHz K^{-2}, $f_{TP} = 7.93 \times 10^{-7}$ GHz (K kPa)$^{-1}$, and $f_{PP} = 3.64 \times 10^{-8}$ GHz kPa^{-2}. Figure 2 also shows frequency dependence of the product of the R_μ functions and the filter function. The magnitude of the difference between a value of $R(\nu, T, P)$ and the value calculated from the series in (7) is less than 4×10^{-5}. For a 755-K filter function $F(\nu)$ all of the functions in (7) are shown in Fig. 2. As a check we have verified that the expansion maintains the Rayleigh–Brillouin function normalization in (2e). In addition the integrals of R_P, R_{PT}, and R_{PP} are all close to zero as they must be, since the right-hand side of (2e) does not depend upon P. We have used ±5 GHz for the limits on the frequency integrals and frequency steps of 0.05 GHz. Typical values of the molecular attenuation factors f_R are 0.3–0.5 GHz, and the accuracy of the values is better than 0.1%. This is adequate to determine temperatures to ±1 K as we shall see later. For temperatures and pressures outside the 245–305-K and 50–100-kPa ranges, this procedure can be repeated using other sets of R_μ functions with different T_0 and P_0 values.

c. *Inversion procedure*

To obtain the temperature from the measured lidar return signals, we assume that the signal count ratios C_1/C_2 in (6) have been measured. Then substitution of (2c), (7), and (8) into (6b) and a three-term expansion of $f_0(T)$ about T_0 yields a quadratic form in $(T - T_0)$ and $(P - P_0)$. The pressure is assumed to have the value P_{ref} at a reference height on the profile so we can solve for the temperature at that height, $T(z)$. Note that P_{ref} need not be the same as our standard pressure P_0. Using the ideal gas law for the equation of state [$n = P/(k_BT)$] gives the density at that level, $n(z)$.

To continue to other altitudes requires the pressure at the adjacent level. Assuming that the atmosphere is in hydrostatic equilibrium implies

$$\frac{\partial P}{\partial z} = -mng, \tag{9}$$

where $g = 9.8$ m s^{-2}. The scale height z_s is defined as $k_BT/mg \approx 8.5$ km. Equation (9) can be written in finite-difference form accurate to first order in $\Delta z/z_s \approx 0.01$ (note $\Delta z \approx \pm 75$ m for our experiment) as

$$P(z + \Delta z) = P(z)\left[\frac{1 - mg\Delta z}{k_BT(z)}\right]. \tag{10}$$

This may be used to calculate the pressure at an adjacent level, $P(z + \Delta z)$. The ratio of the lidar returns from the level at $z + \Delta z$ and (6b) then gives the temperature at that level, $T(z + \Delta z)$. The entire process is repeated for other altitudes to determine the entire profile.

This procedure illustrates the principle; however, because temperature determinations to 1 K require an accuracy of about 1 part in 300, we use an improved approximation to (9) that is accurate to second order $(\Delta z/z_s)^2 \approx 10^{-4}$:

$$P(z + \Delta z) = P(z)\frac{\{1 - mg\Delta z/[2k_BT(z)]\}}{\{1 + mg\Delta z/[2k_BT(z + \Delta z)]\}}. \tag{11}$$

Since this depends upon both $T(z + \Delta z)$ and $P(z + \Delta z)$, one must solve (11) and (6) simultaneously. An iteration converges within two or three steps. In this manner, the profiles of air temperature, pressure, and density can be obtained self-consistently. Note that alternatives to the ideal gas equations of state could be incorporated with little additional difficulty. Also, unlike the method requiring Klett inversion (Kobayashi and Yamada 1988), no assumptions have been made about the aerosol.

We have assumed local thermodynamic equilibrium and the hydrostatic equation. As discussed by Dutton (1976), the atmosphere is expected to be statically stable if the potential temperature does not decrease with altitude. In addition, if the vertical component of the gradient of the horizontal wind is less than about twice the Brunt–Väisälä frequency (about 0.01 s^{-1} at 5 km in the United States standard atmosphere), then the atmosphere is also expected to be stable. Thus our method is most applicable if the potential temperature does not decrease with altitude and if the vertical shear of horizontal wind is small.

d. Sensitivity

Using the preceding inversion procedure, the atmospheric temperature is determined with (6b) by comparing the measured signals to the molecular ratio, f_{m1}/f_{m2}. For a given signal ratio, the intrinsic measurement precision thus depends on the sensitivities of the coefficient ratio, f_{m1}/f_{m2}, to changes in the air temperature and pressure. We define the temperature sensitivity S_{T12} as the fractional change in ratio f_{m1}/f_{m2} for a change in the air temperature of 1 K at $T_0 = 275$ K and $P_0 = 76$ kPa. This sensitivity depends on $F_1(\nu)$ and $F_2(\nu)$ and is given by $S_{T12} = S_{T1} - S_{T2}$, where $S_{Ti} = \delta f_{mi}/f_{mi}$, where

$$\frac{\delta f_{mi}}{f_{mi}} = \frac{\delta f_{Ri} + \gamma\delta f_0}{f_{Ri} + \gamma f_0}, \tag{12}$$

with $\delta f_{Ri} = f_{Ti}\delta T$, and $\delta f_0 = 0.5 f_0 \delta T/T_0$, and $\delta T = 1$ K. (Note that the higher-order corrections in (7) are small for $\delta T = 1$ K.)

Two theoretical models for $F(\nu)$ as well as the measured $F(\nu)$ for barium filters illustrate typical values for S_{T12}. Theoretical forms for $F(\nu)$ are obtained from the absorption line shape of the atomic vapor, $g(\nu)$, as

$$F(\nu) = \exp\left[\frac{-g(\nu)n_{Ba}L\lambda^2A_{21}g_2}{8\pi g_1}\right] = \exp[-Ag(\nu)], \tag{13}$$

where n_{Ba} is the number density of the barium atoms in the filter, L is the effective length of the filter, λ is the wavelength, A_{21} is the Einstein coefficient, and $g_{1(2)}$ is the degeneracy of the barium ground (excited) state. For Gaussian line shapes we have

$$g_G(\nu) = \frac{1}{\Delta\nu_D}\left(\frac{4\ln 2}{\pi}\right)^{1/2}\exp\left[\frac{-4\ln 2(\nu - \nu_0)^2}{(\Delta\nu_D)^2}\right], \tag{14}$$

where ν_0 is the natural transition frequency, the full width at half-maximum of $g(\nu)$ is

$$\Delta\nu_D = \nu_0\left(\frac{8k_BT\ln 2}{Mc^2}\right)^{1/2}, \tag{15}$$

where M is the mass of the barium atom and c is the speed of light.

For filters having Lorentzian line shapes we have

$$g_L(\nu) = \frac{\Delta\nu/2\pi}{(\nu - \nu_0)^2 + (\Delta\nu)^2/4}. \tag{16}$$

The results are summarized in Table 2 where the theoretical filters have 30-dB attenuation at the center and have FWHM of $\Delta\nu_f = 1.7$, 2.1, 2.5, 2.9, or 3.3 GHz. As can be seen, for wide filters, the sharper Gaussian filters have significantly greater temperature sensitivity than the more extended Lorentzian filters. The sensitivities for measured barium filter functions are close to those of the Gaussian filters. Additional information on the barium filters is given by Kuchta et al. (1990).

The choice of filter pairs for temperature measurements, however, involves trade-offs between high temperature sensitivity S_{T12} (i.e., large differences in filter widths) and large signals with little aerosol contamination (i.e., filter widths that are neither too wide nor

TABLE 2. Filter parameters.

Gaussian (with 30-dB attenuation at center)

$\Delta\nu_f$ (GHz)	f_{std} (GHz)	f_T (GHz K^{-1})	$S_T = \delta f_m/f_m$ (K^{-1})	$10^4 f_p$ (GHz kPa^{-1})	$10^4 S_p$ (kPa^{-1})	T_f (K)	$\Delta\nu_D$ (GHz)	A (GHz)
1.7	0.6192	0.0023	0.0036	3.9	6.3	795	0.933	6.86
2.1	0.4680	0.0021	0.0043	2.6	5.0	1210	1.15	8.48
2.5	0.3448	0.0019	0.0052	0.99	2.6	1720	1.37	10.1
2.9	0.2497	0.0016	0.0058	−0.20	−0.69	2310	1.59	11.7
3.3	0.1793	0.0013	0.0063	−0.79	−3.7	3090	1.81	13.3

Lorentzian (with 30-dB attenuation at center)

$\Delta\nu_f$ (GHz)	f_{std} (GHz)	f_T (GHz K^{-1})	$S_T = \delta f_m/f_m$ (K^{-1})	$10^4 f_p$ (GHz kPa^{-1})	$10^4 S_p$ (kPa^{-1})	$\Delta\nu$ (GHz)	A (GHz)
1.7	0.5747	0.0020	0.0034	2.6	4.1	0.567	6.16
2.1	0.4631	0.0018	0.0037	2.2	4.3	0.701	7.60
2.5	0.3740	0.0016	0.0041	1.6	3.8	0.834	9.05
2.9	0.3030	0.0014	0.0043	0.99	3.0	0.968	10.5
3.3	0.2463	0.0012	0.0045	0.59	2.1	1.10	11.9

Experimental barium filter

$\Delta\nu_f$ (GHz)	f_{std} (GHz)	f_T (GHz K^{-1})	$S_T = \delta f_m/f_m$ (K^{-1})	$10^4 f_p$ (GHz kPa^{-1})	$10^4 S_p$ (kPa^{-1})	T_f (K)
1.82	0.5582	0.00212	0.0037	3.29	5.5	750
2.04	0.4644	0.00200	0.0041	2.65	5.3	761
2.51	0.3040	0.00168	0.0051	0.91	2.8	786
2.99	0.1951	0.00131	0.0059	−0.34	−1.4	805
3.25	0.1534	0.00113	0.0063	−0.70	−3.6	811

too narrow). This is intuitively clear and will be discussed quantitatively in the next section. For atmospheric conditions, a pair of barium filters with widths of 2 and 3 GHz is a reasonable choice. The molecular attenuation factor ratio f_{m1}/f_{m2} for this pair will change by 0.19% per kelvin change in the air temperature. The choice of filter temperatures requires knowing f_μ for different widths. Over 200 measurements of filters with widths $\Delta\nu$ ranging from 1.7 to 3.7 GHz were made. Figure 3 shows the expansion coefficients f_μ as a function of filter width. The result of a best fit to these functions are summarized in Table 3. The coefficients of expansions in powers of $\Delta\nu$ are given for f_{std}^{-1} and f_μ/f_{std}, where $\mu = T, P, TT, TP$, and PP. In addition coefficients for $\delta f_m/f_m$ for $\delta T = 1$ K are given.

Three other theoretical models for the Rayleigh–Brillouin line shape have also been used to determine the sensitivity for a pair of barium filters with widths of 1.98 and 3.01 GHz. They are the seven-moment model (SG) of Boley et al. (1972), the model (SH) of Holoway (1966), and the Morse model of Sugawara and Yip (1967), and Sugawara et al. (1968). Figure 4 shows the variation of the expected signal ratio C_1/C_2 calculated from f_{m1}/f_{m2} for an atmospheric pressure of 76 kPa and temperatures between 275 and 295 K. These four models give very nearly the same temperature sensitivity [$S_{T12} = 0.00186$ K^{-1} (six-moment model), 0.00176 K^{-1} (seven-moment model), 0.00192 K^{-1} (Holoway model), and 0.00189 K^{-1} (Morse model)]. However, at a fixed value of $C_1/C_2 = f_{m1}/f_{m2} = 0.42$, the theories gave temperatures 285 K (six-moment model), 284 K (seven-moment model), 287 K (Holoway model), and 278 K (Morse model). Thus over a span of 30 K, the different models would give variations of temperatures within 1 K of the six-moment model, but would be offset by a few degrees. Also shown in Fig. 4 are the results for $C_1/C_2 = f_{R1}/f_{R2}$ if the rotational Raman contribution is eliminated (setting $\gamma = 0$). For a given experimental ratio C_1/C_2, the temperature deduced ignoring the rotational Raman contribution is seen to be much larger (by 45 K) than that obtained by including it (Alvarez et al. 1993).

Similarly we define the pressure sensitivity as $S_{P12} = S_{P1} - S_{P2}$, with $S_{Pi} = f_{Pi}/(f_{stdi} + \gamma f_0)$. From the values in Table 2 for a 2.04-GHz-wide Gaussian filter, we see that a pressure change of 7.7 kPa has the same effect on the on-resonance filter ratio as a 1-K change in the temperature. From another perspective, in going from 2.0 to 2.1 km in the U.S. standard atmosphere (NOAA 1976), the pressure decreases by 0.99 kPa compared to temperature decrease of 0.65 K. This gives $S_P\Delta P/S_T\Delta T = 5.3 \times 10^{-4}/2.7 \times 10^{-3} = 0.2$. Thus, for this filter, the effect on the ratio of the on-resonance lidar signals due to pressure change in moving vertically through the atmosphere is about 20% of the effect due to temperature changes and should not be ignored.

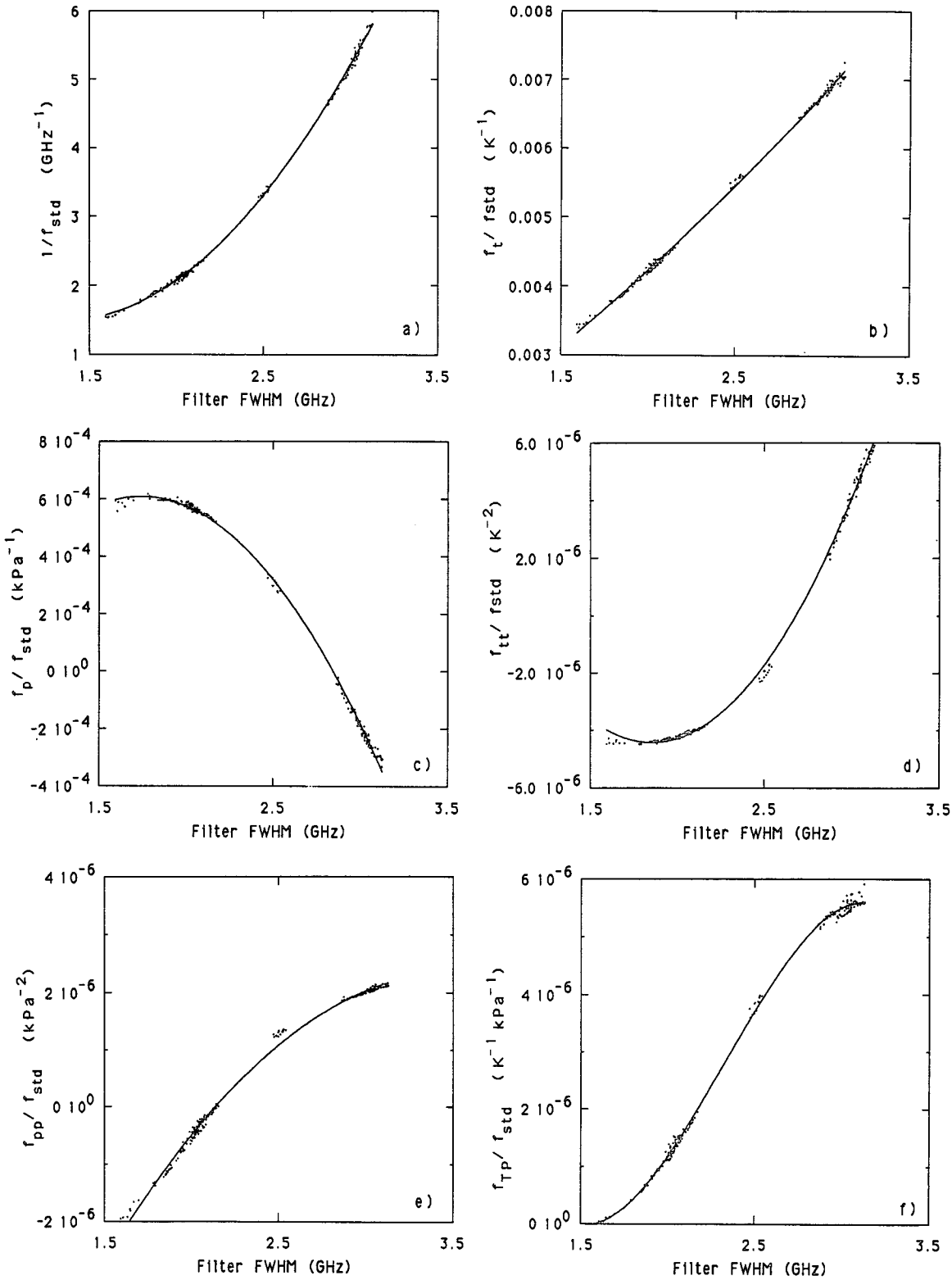

FIG. 3. The expansion coefficients of molecular attenuation factors defined by Eq. (8) for barium vapor filters of different widths. (a) $1/f_{std}$, (b) f_t/f_{std}, (c) f_p/f_{std}, (d) f_{tt}/f_{std}, (e) f_{pp}/f_{std}, and (f) f_{tp}/f_{std}.

TABLE 3. $g(\Delta\nu) = a_0 + a_1\Delta\nu + a_2\Delta\nu^2 + a_3\Delta\nu^3$.

$g(\Delta\nu)$ unit = U	a_0 (U)	a_1 (U GHz^{-1})	a_2 (U GHz^{-2})	a_3 (U GHz^{-3})
$1/f_{std}$ (GHz^{-1})	3.948	−3.655	1.358	0
f_T/f_{std} (K^{-1})	3.810×10^{-4}	1.516×10^{-3}	2.047×10^{-4}	0
f_P/f_{std} (kPa^{-1})	-8.994×10^{-4}	1.732×10^{-3}	-4.974×10^{-4}	0
f_{TT}/f_{std} (K^{-2})	1.784×10^{-5}	-2.403×10^{-5}	6.480×10^{-6}	0
f_{TP}/f_{std} (K kPa^{-1})	2.528×10^{-5}	-3.960×10^{-5}	1.931×10^{-5}	-2.769×10^{-6}
f_{PP}/f_{std} (kPa^{-2})	-1.308×10^{-5}	8.800×10^{-6}	-1.255×10^{-6}	0
$\delta f_m/f_m$ (1)	-6.918×10^{-4}	2.709×10^{-3}	-1.631×10^{-4}	0

Other filters and other atmospheric conditions will give somewhat different percentages, which can be obtained using the information in Tables 2 and 3. Both temperature and pressure variations are included in our iterative procedure.

e. *Precision at a point*

The sensitivity calculation shows that for a proper choice of filter pair, determining the temperature to 1 K requires determining the signal strength to roughly 0.2%. Possible sources of uncertainties in temperature determinations using (6b) include fluctuations in the measured signal ratio $\delta(C_1/C_2)$, errors in the estimation of atmospheric pressure δP_{air}, and the variations of the filter functions and thus the ratio $\delta(f_{std1}/f_{std2})$ during data acquisition. In terms of these fluctuations, the temperature measurement uncertainty δT_{air} may be expressed as

$$\delta T_{air} = \frac{1}{S_{T12}}\left[-S_{P12}\delta P_{air} - \delta \ln\left(\frac{f_{std1}}{f_{std2}}\right) + \delta \ln\left(\frac{C_1}{C_2}\right)\right]. \tag{17}$$

Since the fluctuations of these terms are independent, we consider their effects on the temperature measurement separately.

First consider the effect of δP_{air}. An incorrect assessment of the air pressure will lead to an error in the temperature of $\delta T_{air} = -S_{P12}\delta P_{air}/S_{T12}$ which, for the filter pair discussed above, gives a temperature error of only 1 K for a relatively large pressure error of 7.7 kPa = 76 mb.

Second consider the effect of $\delta(f_{std1}/f_{std2})$ due to the variations of the filter functions during data acquisition. Fluctuations in the filter function $F(\nu)$ may be due to the variations of the temperature and vapor density in the filter during the experiment. These fluctuations will be reflected in changes in the FWHM, $\Delta\nu_f$, which gives

$$\delta \ln\left(\frac{f_{std1}}{f_{std2}}\right) = \frac{\delta(f_{std1})}{(f_{std1})} - \frac{\delta(f_{std2})}{(f_{std2})}, \tag{18}$$

where

$$\frac{\delta f_{std}}{f_{std}} = \frac{1}{f_{std}}\frac{\partial f_{std}}{\partial \Delta\nu_f}\delta(\Delta\nu_f). \tag{19}$$

We have made over 700 measurements of barium filter functions $F(\nu)$ for the current setup and have obtained the $\Delta\nu_f$ and f_{std} with the results shown in Fig. 5. A fit to the data for $1.7 \leqslant \Delta\nu_f \leqslant 3.7$ GHz gives $f_{std} = 1.7204 - 0.8372\Delta\nu + 0.1091\Delta\nu^2$. Thus the coefficient of $\delta(\Delta\nu)$ on the right-hand side of (19) may be calculated and the negative of it is also shown on Fig. 5. For filters with widths between 2 and 3.3 GHz, the coefficient is between −0.8 and −1 GHz^{-1} so $\delta f_{std}/f_{std} \approx -\delta(\Delta\nu)$ GHz^{-1} and

$$\delta T_{air} \approx \frac{\delta(\Delta\nu_1) - \delta(\Delta\nu_2)}{S_{T12}\ \text{GHz}}. \tag{20}$$

Widths may vary due to variations in the filter temperatures. Controlling the filter temperature to better than 1 K is difficult at the typical temperature used in the barium filter ($\sim$780 K $\approx$ 950F). We find a typical variation in filter widths of 16 MHz over five consecutive runs. The sensitivity factor S_{T12} ranges from 0.0003 to 0.003 K^{-1} depending on the filter pair used. For two filters with widths 2.04 and 2.99 GHz (temperatures of about 766 and 811 K), $S_{T12} = 0.002$ K^{-1}

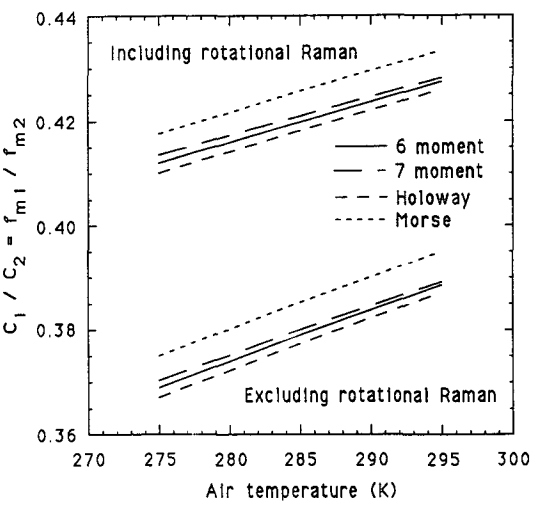

FIG. 4. Ratio of scattered signal passing through two different barium filters (widths 1.98 and 3.01 GHz) as calculated using the Rayleigh–Brillouin scattering function $R(\nu, T, P)$ from four different kinetic theory models. The upper curves include the rotational Raman contribution and the lower curves do not.

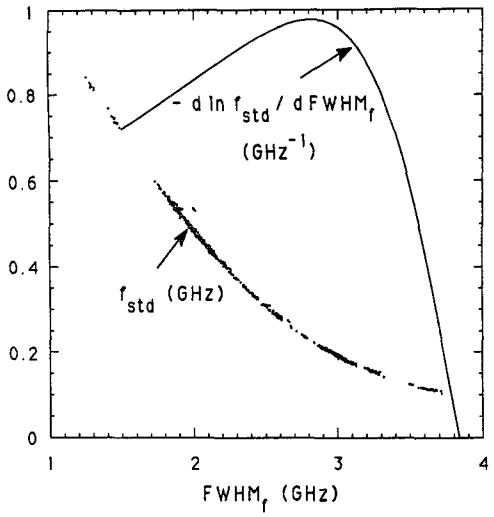

FIG. 5. Plot of $f_{std} = \int F(\nu)R_{std}(\nu)d\nu$ for filters of different widths. Also shown is the variation of -1 times the logarithmic derivative of that quantity with respect to the filter widths.

and the filter width variation can lead to an error of about 8 K in the air temperature. This uncertainty agrees with the observed uncertainties in our field experiments. Recently Voss and Weitkamp (1992) have shown for lead vapor filters at 283.306 nm that by varying the length, temperature, and isotopic content one can optimize the filters. Two such filters within one oven will have much less sensitivity to the oven temperature than will typical filters such as ours.

Third, consider the effect due to signal fluctuations, $\delta(C_1/C_2)(C_1/C_2)^{-1}$. To achieve the intrinsic uncertainty due to the filter variations, we integrate long enough so that $\delta \ln(C_1/C_2) < \delta \ln(f_{std1}/f_{std2})$. Since the effect of δP_{air} is also likely to be small, the uncertainties caused by the variation of the filter transmission function could be made to dominate the measured precision at a point.

Finally, we consider the effect of background sky light. This light is reduced by the presence of the interference filter that may have a bandpass of a few nanometers. The background light that does get through will be constant in time and can be further eliminated by subtracting the signal measured between pulses. An error in the background subtraction by a number of counts δN_B will lead to a temperature offset of $\delta N_B/(NS_{T12})$. Thus 1-K accuracy will be maintained for regions where the number of counts N is greater than $\delta N_B/S_{T12}$, where $1/S_{T12}$ is approximately 500 for pairs of 2- and 3-GHz atomic filters. Typically for our setup this source of error is unimportant for ranges within 5 km.

f. Precision over the profile

We have seen in (17) how the uncertainties in the pressure affect the determination of the temperature at a single point. We now turn to the possibility of errors propagating from one altitude to another through the hydrostatic equilibrium condition, (9). We consider the calculation of the pressure from the first- and second-order-accurate approximations, Eqs. (10) and (11). For the simple case of an isothermal atmosphere, $T(z) = T_{ref}$, the first order (10) gives

$$P_k = P_{ref}\left(1 - \frac{\Delta z}{z_s}\right)^k \approx P_{exact,k}\left[1 - \frac{k}{2}\left(\frac{\Delta z}{z_s}\right)^2 + \cdots\right], \tag{21}$$

where k is the bin number, $z = k\Delta z$, $\Delta z = 75$ m, and z_s is roughly 8500 m. The exact solution to (9) is

$$P_{exact,k} = P_{ref}\exp\left(\frac{-k\Delta z}{z_s}\right). \tag{22}$$

Thus over a distance of 20 km $= k\Delta z$, the error in pressure is 1% for the first-order-accurate calculation. The second-order-accurate (11) gives

$$P_k = P_{ref}\left(1 - \frac{\Delta z}{2z_s}\right)^k\left(1 + \frac{\Delta z}{2z_s}\right)^{-k}$$

$$\approx P_{exact,k}\left[1 - \frac{k}{12}\left(\frac{\Delta z}{z_s}\right)^3 + \cdots\right]. \tag{23}$$

Over a distance of 20 km, the error in pressure is only 0.01% for the second-order-accurate calculation. Use of the second-order equation should insure minimal propagation of errors over all distances of interest for the troposphere.

g. Aerosol properties

After determining the temperature, pressure, and molecular density profiles, the aerosol properties can be obtained. The backscatter ratio is defined (Kobayashi 1987) as the ratio of the total backscattering coefficient, $\beta_m + \beta_a$, to the backscatter due to the air molecules, β_m,

$$r_\beta = \frac{\beta_m + \beta_a}{\beta_m}. \tag{24}$$

In terms of the measured signals, (2a) and (3), this becomes

$$r_\beta = \frac{N_{off}\mathcal{P}_{on}}{N_{on}\mathcal{P}_{off}}\frac{f_m(T, P)}{f_0(T, P)}. \tag{25}$$

Note that, due to the f_m and f_0 factors, the atmospheric temperature and pressure are required in addition to the ratios of the signals, and the laser powers. Obviously, the backscatter ratio can be determined from the measured signals from either channel, giving identical results as long as (6) is satisfied. The ratio of the laser powers $\mathcal{P}_{on}/\mathcal{P}_{off}$ would be the same for both channels.

The extinction coefficient profile $\alpha(z)$ may be obtained from (2) as

$$\alpha(\nu, z) = \frac{1}{2}\frac{d}{dz}\ln\left[\frac{1}{N_{on}z^2}\xi_{on}(\nu, z)\beta_m(z)\frac{f_m}{f_0}\right], \quad (26a)$$

or equivalently, by (25)

$$\alpha(\nu, z) = \frac{1}{2}\frac{d}{dz}\ln\left[\frac{1}{N_{off}z^2}\xi_{off}(\nu, z)r_\beta\beta_m(z)\right]. \quad (26b)$$

For these calculations, the z dependence of the telescope overlap function $\xi_{on}(z)$ and $\xi_{off}(z)$ must be known. In practice, these overlap functions $\xi_{on}(z)$ and $\xi_{off}(z)$ to a good approximation are independent of z for ranges beyond 0.5 km in our case. The profile of aerosol extinction coefficient and extinction ratio, α_a and r_α, respectively, may be evaluated using (26a) or (26b) beyond this point by

$$\alpha_a = \alpha(\nu, z) - n(T, P)\sigma, \quad (27a)$$

and

$$r_\alpha = \frac{\alpha}{n(z)\sigma}, \quad (27b)$$

where the extinction ratio is defined as the ratio of total extinction coefficient to that of molecular scattering. Unlike the backscatter ratio determination, the knowledge of $\mathcal{P}_{on}/\mathcal{P}_{off}$ is not needed for the evaluation of α and r_α.

Finally the backscattering phase function defined as

$$PF = \frac{\beta_a}{\alpha_a}, \quad (28)$$

depends on the distribution of aerosol sizes and shapes. It can be obtained as

$$PF(z) = n(T, P)\frac{d\sigma}{d\Omega}(r_\beta - 1)[\alpha(z) - n(T, P)\sigma]^{-1}, \quad (29)$$

where the Rayleigh scattering cross section including both central and rotational fine structure for air is (Measures 1984)

$$\sigma = \frac{8\pi}{3}\frac{d\sigma}{d\Omega}, \quad (30a)$$

and

$$\frac{d\sigma}{d\Omega} = \left[\frac{550}{\lambda(\text{nm})}\right]^4 5.45 \times 10^{-28}\ \text{cm}^2\ \text{sr}^{-1}. \quad (30b)$$

h. Experimental procedure

To experimentally determine the profiles of atmosphere and aerosol properties, a typical sequence of experiments consists of (a) laboratory scan of filter transmissions (vapor temperatures T_1 and T_2) giving $F_1(\nu)$ and $F_2(\nu)$ [see (1)], (b) lidar return with laser tuned off-resonance giving $N_{1off}(z)$ and $N_{2off}(z)$, [see (5)], and (c) lidar return with laser tuned on-resonance giving $N_{1on}(z)$ and $N_{2on}(z)$ [see (4)]. In carrying out the measurements of (b) and (c), the outgoing laser power is simultaneously monitored. Results of field experiments will be reported as a companion paper (Alvarez et al. 1993).

4. Summary and conclusions

We have discussed the use of high spectral resolution lidar for the determination of atmospheric temperature profiles. Blocking the aerosol contribution requires a filter that has a full width at half maximum of 1.7–3.5 GHz and a maximum attenuation of at least 30 dB. To determine temperatures to 1 K requires measuring the ratio of two on-resonance signals to about 0.2%. For a barium vapor filter this will require holding the vapor temperature to about 0.1 K at a temperature of about 800 K. Fluctuations in the filter temperature also could lead to difficulty in measuring an accurate filter transmission function. This sensitivity to filter temperature can be reduced by designing matched filters of different lengths that are placed in a common oven. We have shown that the vertical profiles of atmospheric and aerosol parameters can be determined directly from inverting Rayleigh–Mie lidar data using atomic blocking filters and an inversion procedure outlined in this paper if the pressure at *a single reference level* is independently provided. It is clear from Table 1 that our lidar technique can provide more information than any other existing lidar schemes.

Acknowledgments. This project was supported in part through Contract DAAL03-86-K-0175 to the U.S. Army Center for Geosciences at Colorado State University where R. J. Alvarez, II, was and L. M. Caldwell is a Geoscience Fellow.

REFERENCES

Alvarez, R. J., II, L. M. Caldwell, Y. H. Li, D. A. Krueger, and C. Y. She, 1990: High-spectral-resolution lidar measurement of tropospheric backscatter-ratio with barium atomic blocking filters. *J. Atmos. Oceanic Technol.*, **7**, 876–881.

——, L. M. Caldwell, P. G. Wolyn, D. A. Krueger, T. B. McKee, and C. Y. She, 1993: Profiling temperature, pressure, and aerosol properties using a high spectral resolution lidar employing atomic blocking filters. *J. Atmos. Oceanic Technol.*, **10**, 546–556.

Ansmann, A., M. Riebesell, and C. Weitkamp, 1990: Measurement of atmospheric aerosol extinction profiles with a Raman lidar. *Opt. Lett.*, **15**, 746–748.

Arshinov, F., S. M. Bobrovnikov, V. E. Zuev, and V. M. Mitev, 1983: Atmospheric temperature measurements using a pure rotational Raman lidar. *Appl. Opt.*, **22**, 2984–2990.

Bates, R. D., 1984: Rayleigh scattering by air. *Planet. Space Sci.*, **32**, 785–790.

Boley, C. D., R. C. Desai, and G. Tenti, 1972: Kinetic models and Brillouin scattering in a molecular gas. *Can. J. Phys.*, **50**, 2158–2173.

Cooney, J., 1972: Measurement of atmospheric temperature profiles by Raman backscatter. *J. Appl. Meteor.*, **11,** 108–112.

——, 1984: Atmospheric temperature measurement using a pure rotational Raman lidar: Comment. *Appl. Opt.*, **23,** 653–654.

Dutton, J. A., 1976: *The Ceaseless Wind; An Introduction to the Theory of Atmospheric Motion.* McGraw-Hill, 579 pp.

Endemann, M., and R. L. Byer, 1981: Simultaneous remote measurements of atmospheric temperature and humidity using a continuously tunable IR lidar. *Appl. Opt.*, **20,** 3211–3217.

Evans, B. T. N., 1988: Sensitivity of the backscatter/extinction ratio to changes in aerosol properties: Implications for lidar. *Appl. Opt.*, **27,** 3299–3305.

Fiocco, G., G. Beneditti-Michelangeli, K. Maischberger, and E. Madonna, 1971: Measurement of temperature and aerosol to molecule ratio in the troposphere by optical radar. *Nature, Phys. Sci.*, **229,** 78–79.

Grund, C. J., and E. W. Eloranta, 1988: High spectral resolution lidar measurement of cirrus cloud optical and physical properties. *Extended Abstracts, 14th Int. Laser Radar Conf.*, Innichen–San Candido, Italy, Int. Comm. on Laser Atmos. Studies, Int. Radiation Comm., and Int. Assoc. of Meteorology and Atmos. Physics, 28–31.

Holoway, 1966: New statistical models for kinetic theory: Methods of construction. *Phys. Fluids,* **9,** 1658–1673.

Kalshoven, J. E., Jr., C. L. Korb, G. K. Schwemmer, and M. Dombroski, 1981: Laser remote sensing of atmospheric temperature by observing resonant absorption of oxygen. *Appl. Opt.*, **20,** 1967–1971.

Keckhut, P., M. L. Chanin, and A. Hauchecome, 1990: Stratosphere temperature measurement using Raman lidar. *Appl. Opt.*, **29,** 5182–5185.

Klett, J. D., 1981: Stable analytical inversion solution for processing lidar returns. *Appl. Opt.*, **20,** 211–220.

——, 1986: Extinction boundary value algorithms for lidar inversion. *Appl. Opt.*, **25,** 2462–2464.

Kobayashi, T., 1987: Techniques for laser remote sensing of environment. *Remote Sens. Rev.*, **3,** 1–56.

——, and T. Yamada, 1988: Tropospheric temperature sensing by the Raman and Rayleigh–Mie Lidar using UV excimer lasers. *Extended Abstracts, 14th Int. Laser Radar Conf.*, Innichen–San Candido, Italy, Int. Comm. on Laser Atmos. Studies, Int. Radiation Comm., and Int. Assoc. of Meteorology and Atmos. Physics, 67–69.

Kuchta, E., R. J. Alvarez, II, Y. H. Li, D. A. Krueger, and C. Y. She, 1990: Collisional broadening of Ba I line (553.5 nm) by He or Ar. *Appl. Phys.*, **B50,** 129–132.

Lehmann, F. J., S. A. Lee, and C. Y. She, 1986: Laboratory measurements of atmospheric temperature and backscatter ratio using a high-spectral-resolution lidar technique. *Opt. Lett.*, **11,** 563–565.

Mason, J. B., 1975: Lidar measurement of temperature: A new approach. *Appl. Opt.*, **14,** 76–78.

Measures, R. M., 1984: *Laser Remote Sensing: Fundamentals and Applications.* John Wiley & Sons, 510 pp.

Melfi, S. H., 1972: Remote measurements of the atmosphere using Raman scattering. *Appl. Opt.*, **11,** 1605–1610.

Murray, E. R., D. D. Powell, and J. E. van der Laan, 1980: Measurement of average atmospheric temperature using a CO_2 laser radar. *Appl. Opt.*, **19,** 1794–1797.

NOAA, 1976: United States National Oceanic and Atmospheric Administration. *U.S. Standard Atmosphere 1976,* U.S. Govt. Printing Office, 227 pp.

Penney, C. M., R. L. Peters, and M. Lapp, 1974: Absolute rotational Raman cross sections for N_2, O_2, and CO_2. *J. Opt. Soc. Am.*, **64,** 712–716.

Schwemmer, G. K., and T. D. Wilkerson, 1979: Lidar temperature profiling: Performance simulations of Mason's method. *Appl. Opt.*, **18,** 3539–3541.

Schwiesow, R. L., and L. Lading, 1981: Temperature profiling by Rayleigh-scattering lidar. *Appl. Opt.*, **20,** 1972–1979.

Shardanand, and A. D. Prasad-Rao, 1977: Absolute Rayleigh scattering cross sections of gases and freons of stratospheric interest in the visible and ultraviolet regions. NASA Tech. Note, TN D-8442, 37 pp.

She, C. Y., 1990: Remote measurement of atmospheric parameters: New applications of physics with lasers. *Contemp. Phys.*, **31,** 247–260.

——, Alvarez, R. J., II, L. M. Caldwell, and D. A. Krueger, 1992: High-spectral-resolution Rayleigh–Mie lidar measurement of aerosol and atmospheric profiles. *Opt. Lett.*, **17,** 541–543.

Shimizu, H., S. A. Lee, and C. Y. She, 1983: High spectral resolution lidar system with atomic blocking filters for measuring atmospheric parameters. *Appl. Opt.*, **22,** 1373–1381.

Shipley, S. T., D. H. Tracy, E. W. Eloranta, J. T. Tauger, J. T. Sroga, F. L. Roesler, and J. A. Weinman, 1983: High spectral resolution lidar to measure optical scattering properties of atmospheric aerosols. 1: Theory and instrumentation. *Appl. Opt.*, **22,** 3716–3724.

Sugawara, A., and S. Yip, 1967: Kinetic model analysis of light scattering by molecular gases. *Phys. Fluids,* **10,** 1911–1921.

——, S. Yip, and L. Sirovich, 1968: Spectrum of density fluctuations in gases. *Phys. Fluids,* **11,** 925–932.

Tenti, G., C. D. Boley, and R. C. Desai, 1974: On the kinetic model description of Rayleigh–Brillouin scattering from molecular gases. *Can. J. Phys.*, **52,** 285–290.

Voss, E., and C. Weitkamp, 1992: Investigations on atomic-vapor-filter high-spectral-resolution lidar for temperature measurements. *Proc. 16th. Int. Laser Radar Conf.*, Cambridge, MA, U.S. Air Force Office of Sci. Res., NASA Langley Research Center, U.S. Air Force Phillips Laboratory, Amer. Meteor. Soc., and the Optical Soc. of Amer., NASA Conf. Pub. 3158, Parts 1 and 2, 699–702.

Young, A. T., 1982: Rayleigh scattering. *Physics Today,* **35,** 42–48.